Frontiers in Bioscience Landmark

Front. Biosci. (Landmark Ed) **2023**; 28(6): 131
https://doi.org/10.31083/j.fbl2806131

Original Research

CRISPR/Cas9-Mediated Gene Correction in Osteopetrosis Patient-Derived iPSCs

Dandan Li[1,2,†], Minglin Ou[1,3,†], Wei Zhang[1,2], Qi Luo[1], Wanxia Cai[1], Chune Mo[3], Wenken Liang[3], Guandong Dai[4], Lianghong Yin[2], Peng Zhu[4,*], Donge Tang[1,*], Yong Dai[1,*]

[1]Clinical Medical Research Center, The Second Clinical Medical College of Jinan University (Shenzhen People's Hospital), 518020 Shenzhen, Guangdong, China
[2]Institute of Nephrology and Blood Purification, The First Affiliated Hospital, Jinan University, 510632 Guangzhou, Guangdong, China
[3]Central Laboratory, Guangxi Health Commission Key Laboratory of Glucose and Lipid Metabolism Disorders, The Second Affiliated Hospital of Guilin Medical University, 541001 Guilin, Guangxi, China
[4]Clinical Lab of Shenzhen Pingshan People's Hospital, Shenzhen Pingshan People's Hospital, 518118 Shenzhen, Guangdong, China
*Correspondence: gdszpsrmyy@163.com (Peng Zhu); donge66@126.com (Donge Tang); daiyong22@aliyun.com (Yong Dai)
[†]These authors contributed equally.
Academic Editor: Elisa Belluzzi
Submitted: 20 December 2022 Revised: 5 March 2023 Accepted: 14 March 2023 Published: 30 June 2023

Abstract

Background: Osteopetrosis represents a rare genetic disease with a wide range of clinical and genetic heterogeneity, which results from osteoclast failure. Although up to 10 genes have been identified to be related with osteopetrosis, the pathogenesis of osteopetrosis remains foggy. Disease-specific induced pluripotent stem cells (iPSCs) and gene-corrected disease specific iPSCs provide a platform to generate attractive *in vitro* disease cell models and isogenic control cellular models respectively. The purpose of this study is to rescue the disease causative mutation in osteopetrosis specific induced pluripotent stem cells and provide isogenic control cellular models. **Methods**: Based on our previously established osteopetrosis-specific iPSCs (ADO2-iPSCs), we repaired the point mutation R286W of the *CLCN7* gene in ADO2-iPSCs by the clustered regularly interspaced short palindromic repeats (CRISPR)/CRISPR-associated protein 9 (Cas9) mediated homologous recombination. **Results**: The obtained gene corrected ADO2-iPSCs (GC-ADO2-iPSCs) were characterized in terms of hESC-like morphology, a normal karyotype, expression of pluripotency markers, homozygous repaired sequence of *CLCN7* gene, and the ability to differentiate into cells of three germ layers. **Conclusions**: We successfully corrected the point mutation R286W of the *CLCN7* gene in ADO2-iPSCs. This isogenic iPSC line is an ideal control cell model for deciphering the pathogenesis of osteopetrosis in future studies.

Keywords: CRISPR/Cas9; gene correction; osteopetrosis; iPSCs; *CLCN7*

1. Introduction

Osteopetrosis represents a rare genetic disease which results from osteoclast failure [1,2]. The clinical manifestations are heterogeneous and range from asymptomatic to severe [3]. The typical feature of osteopetrosis is an increased skeletal mass [2]. In the intermediate/severe forms, patients also present with osteomyelitis, anemia with extramedullary hematopoiesis, cranial nerve involvement, short stature, malformations and brittle bones [4]. Based on genetic pattern, osteopetrosis is classified into autosomal recessive osteopetrosis (ARO), autosomal dominant osteopetrosis (ADO) and X-linked osteopetrosis, in which, ADO is the most frequent form of osteopetrosis with a global incidence of 5/100,000 [5,6]. To date, the genes identified to affect osteopetrotic patients are all involved in the function of the osteoclast, including *LRP5*, *CLCN7*, *TCIRG1*, *TNFS11*, *CAII*, *OSTM1*, *PLEKHM1*, *TNFRS11A*, *SNX10*, *NEMO* [7]. Although some palliative treatments are utilized for osteopetrosis treatment [4], such as pain infections could be treated using analgesics and antibiotics, multiple fractures could be treated by surgery, and hematopoiesis cloud be improved by erythropoietin and glucocorticoids [4], there is no cure for osteopetrosis. Hematopoietic stem cell transplantation (HSCT) provides severe patients an effective therapy to improve the quality of their life [4]. However, as it currently stands, HSCT has many limitations and its lethal complications have hampered its applicability for ADO patients [8,9]. Therefore, advanced basic research which is focused on the pathogenesis of osteopetrosis should be performed to provide innovative orientations for therapeutic approaches to osteopetrosis.

Induced pluripotent stem cells (iPSCs), which possess infinite proliferative activity, exhibit multipotent differentiation potential and harbor the genetic information from their parental cells, have provided a previously unattainable platform to generate attractive *in vitro* cell models that could accurately mirror diseases phenotypic manifestations [10]. Due to the promises of iPSCs, an increasing number of disease-specific iPSCs or control iPSCs have been

derived from somatic cell samples from patients or control individuals respectively [11]. Differentiated targeted cells of interest that can manifest disease features have been employed to discover pathophysiological conditions. Gene corrected disease-specific iPSCs on causative mutation(s) exhibit rescued phenotypes, which have unlocked new possibilities to delve disease mechanisms as a resource of isogenic control cellular models [12,13]. Among the reported genome engineering technologies, clustered regularly interspaced short palindromic repeats-associated 9 (CRISPR/Cas9) technology possesses the capacity to precisely modify genes [14,15]. The reported research using CRISPR/Cas9 to correct the mutations in patient-specific iPSCs revealed that the combination of patient-specific iPSCs with CRISPR/Cas9 holds a substantial promise to elucidate the role of targeted genes in the pathophysiology of diseases [16–19].

Previously, we have reported an osteopetrosis family carrying a heterozygous mutation, c.856C>T (p.R286W) in *CLCN7* exon 10 and generated osteopetrosis-specific iPSCs (ADO2-iPSCs) [20]. We also performed integrated proteome and lysine 2-hydroxyisobutyrylome analysis on ADO2-iPSCs [20]. Here we utilized the CRISPR/Cas9 system to successfully correct the *CLCN7* mutation in ADO2-iPSCs, where the mutated triplet TGG (tryptophan) was corrected to the wild-type triplet CGG (arginine). We confirmed by sequencing analysis that the mutation was corrected without further deletions or insertions at the CRISPR cutting site. The gene corrected ADO2-iPSCs (GC-ADO2-iPSCs) had a normal karyotype, exhibited iPSC-like morphology, expressed pluripotency markers and differentiated into cells representative of the three embryonic germ layers.

2. Method

2.1 Animal Study and Cell Line Source

Animal studies were approved by Guilin Medical University Laboratory Animal Ethics Committee (Approval No. GLMC 202003175). Four weeks-old SCID Beige mice were purchased from the Beijing Vital River Laboratory Animal Technology Co., Beijing, China and kept in the central laboratory of the Second Affiliated Hospital of Guilin Medical University. Mice were sacrificed by cervical dislocation. The criteria for euthanizing animals prior to the planned end of the experiment: (1) Animals are on the verge of death or unable to move, (2) Dyspnea, (3) Diarrhea or incontinence, (4) The body weight of animals decreased by 20% of that before the experiment, (5) Inability to eat or drink, (6) Experimental animals show obvious anxiety, restlessness, or tumor weight exceeding 10% of the animal's own body weight, (7) Experimental animals show paralysis, persistent epilepsy or stereotyped behavior, (8) The skin damage area of animals accounts for more than 30% of the whole body, or there is infection and purulence. All mice need to be sacrificed at the conclusion of the experiment. The cell line ADO2-iPSC used in this study was reported in our previous work [20] and stored in the central laboratory of the Second Affiliated Hospital of Guilin Medical University. The ADO2-iPSCs cell line is negative for mycoplasma. The identical STR profiles were confirmed between ADO2-iPSCs and the proband [20]. The construction of ADO2-iPSCs was approved by the Medical Ethics Committee of Shenzhen Peoples Hospital (the Second Clinical Medical College of Jinan University) and informed consent was obtained from the participant donor [20].

2.2 Single-Guide RNA Design and Genome Editing

CRISPR/Cas9-mediated homology-directed repair (HDR) technology was employed for single base correction at the *CLCN7* locus in ADO2-iPSC line. The single-guide RNA (sgRNA) sequences were designed using the online tool (http://www.deephf.com/index/#/cas9) to target *CLCN7* mutant sequence (c.856C>T, p.R286W). One sgRNA that overlap the patient-specific mutation was selected. The sgRNA sequence was constructed on Cas9 expressing plasmid vectors (pSpCas9n(BB)-2A-GFP (px461), Addgene plasmid#48140) [21]. The donor homologous arm sequence targeting *CLCN7* was cloned into the pUC57 plasmid. Detailed sgRNA and donor sequences are shown in **Supplementary Fig. 1**. For gene editing, 1×10^5 dissociated ADO2-iPSCs were electroporated with 0.25 µg sgRNA plasmid and 0.75 µg donor plasmid using the Amaxa Nucleofector II device, Nucleofector 2b (Lonza, Cologne, Germany) transfection system with Neon transfection kit (no. MPK1096, ThermoFisher Scientific, Waltham, MA, USA) at 1050 V, 5 ms, one pulse. Following electroporation, the iPSCs were maintained in Nuwacell hiPSC/hESC medium (no. RP01020, Nuwacell Biotechnologies Co., Ltd., Hefei, Anhui, China) supplemented with 0.75 µg/mL blebbistain (no. RP01008, Nuwacell Biotechnologies Co., Ltd., Hefei, Anhui, China) for 6–8 h. Then blebbistain was removed from the medium. Twenty-four hours post electroporation, transfected iPSCs were treated with 2 µg/mL of blasticidin (no. ant-bl-05, InvivoGen, Carlsbad, CA, USA) at 37 °C in 5% CO_2 for 7–10 days. The media was changed daily and cells were passaged when 80% confluency was reached. After blasticidin selection, the iPSCs were plated at a low density in 6-well plates and expanded until iPSC colonies were ready to be picked.

2.3 The Amplification of sgRNA Fragment

A polymerase chain reaction (PCR) method was carried out for sgRNA fragment amplification. The total volume of amplification reaction was 30 µL consisting of 18 µL of ddH_2O, 3 µL of each primer (F5′-CACCGCGCAGAGACACAGAGAAGT-3′ and R5′-AAACACTTCTCTGTGTCTCTGCGC-3′), 6 µL of 5X Phusion HF Buffer (no. F-520L, Thermo Fisher Scientific, Waltham, MA, USA). The annealing conditions were listed in Table 1.

Table 1. The annealing conditions for sgRNA fragment amplification.

Step	Temperature	Ramp Rate	Time
Initial Denaturation	95 °C	–2.4 °C/s	10 min
Annealing	95 °C–85 °C	–0.3 °C/s	
	85 °C		1 min
	85 °C–75 °C	–0.3 °C/s	
	75 °C		1 min
	75 °C–65 °C	–0.3 °C/s	
	65 °C		1 min
	65 °C–55 °C	–0.3 °C/s	
	55 °C		1 min
	55 °C–45 °C	–0.3 °C/s	
	45 °C		1 min
	45 °C–35 °C	–0.3 °C/s	
	35 °C		1 min
	35 °C–25 °C	–0.3 °C/s	
	25 °C		1 min
Hold	4 °C		Hold

2.4 DNA Isolation

The subclones of iPSCs were collected and total DNA was isolated using the QuickExtract™ DNA Extraction Solution 1.0 (no. QE09050, Epicentre, Madison, WI, USA) according to the manufacturer's instructions. Briefly 500–1000 cells were collected and transferred into 50 µL of rapid extraction buffer and mixed by vortexing for 15 seconds. The mixture was incubated at 64 ℃ for 6 minutes and 98 ℃ for 2 minutes. The DNA was stored at –20 ℃ for up to 1 week, or at –70 ℃ for longer periods.

2.5 Nested-PCR and Sanger Sequencing

A nested PCR method was carried out in this study. The total volume of amplification reaction was 50 µL consisting of 15 µL of ddH_2O, 2.5 µL of each primer, 25 µL of Q5 High-Fidelity 2X Master Mix (no. M0491, New England Biolabs, Ipswich, MA, USA), and 5 µL of DNA template. The DNA genome sample and the external primer pair (F5′ TCCCTTTCTGAGAGCCGTG 3′ and R5′ GTGGAGAGCAAGAGGGGAAG 3′) were used at the first amplification. The product after primary amplification was expected to 815 bp. For the nested PCR assay, the amplification product obtained by the first-step PCR was re-amplified. The internal primer pair (F5′ TCCCTTTCTGAGAGCCGTG 3′ and R5′ AGGACCAAGGGCGAACTG 3′) was used. The expected product size after secondary amplification was 724 bp. The cycling conditions for both rounds of PCR amplification were same, which included an initial denaturation at 98 ℃ for 30 s, followed by 35 cycles of 95 ℃ for 5–20 s, 65 ℃ for 20 s, 72 ℃ for 30 s and a final extension at 72 ℃ for 2 min. The nested PCR product was analyzed by agarose gel electrophoresis. For sanger sequencing, the targeted PCR product was sequenced using an ABI 3100 DNA analyzer. The results were analyzed using Chromas software (version 1.62, www.technelysium.com.au/chromas.html).

2.6 Karyotype Analysis

G-banding karyotype analysis was performed for karyotyping iPSC lines [20]. The iPSCs were harvested at 80% confluency and treated with 50 ng/mL colchicine for 2 h at 37 ℃. The single-cell suspension of iPSCs was swollen by exposure to KCl hypotonic solution (0.075 M) and fixed in 3:1 methanol to acetic acid. A minimum of 30 metaphase spreads were analyzed for each sample. The samples were examined and photographed using Lieca GSL120 (Leica Biosystems, Richmond, IL, USA).

2.7 Western Blot

Total proteins were extracted using RIPA lysis buffer (no. KGP702-100, KeyGEN BioTECH, Nanjing, Jiangsu, China), and the protein concentration was determined using BCA assay. The same amount of protein (20 µg) from each sample was loaded to SDS-PAGE and transferred to nitrocellulose membranes. Following blocking with 5% skimmed milk for 2 h at room temperature, the membranes were first incubated with primary antibodies against CLCN7 (no. DF3932, Affinity Biosciences, Melbourne, Victoria, Australia, dilution, 1:1000) or β-actin (no. AF5003, Beyotime Institute of Biotechnology, Shanghai, China, dilution, 1:2000) at 4 ℃ overnight and then with goat anti-rabbit IgG (H + L) secondary antibody (no. 31460100, Thermo Fisher Scientific, Waltham, MA, USA, dilution, 1:10,000) at room temperature for 2 h. Finally, the immunoblots were visualized using a Quantity One system image analyzer (Bio-Rad Laboratories, Hercules, CA, USA) and the bands of proteins were evaluated using ImageJ software (version 1.53t, National Institute of Mental Health, Bethesda, MD, USA, https://imagej.nih.gov/ij/).

2.8 Flow Cytometric Analysis

Flow cytometric analysis was used for pluripotency validation [20]. GC-ADO2-iPSCs were dissociated with Solase dissociation buffer (no. RP01021, Nuwacell Biotechnologies Co., Ltd., Hefei, Anhui, China) and incubated with the antibodies for SSEA-4 (no. 560128, BD Pharmingen, San Diego, CA, USA) or TRA-1-81 (no. 560161, BD Pharmingen, San Diego, CA, USA) at 4 ℃ for 20 min in dark. Samples were then analyzed using a FACScan flow cytometry (BD Biosciences, San Diego, CA, USA), and data were analyzed using the FlowJo Software (version 7.6.5, FlowJo LLC, Ashland, OR, USA).

2.9 Teratoma Assay

Teratoma assay was performed to evaluate the pluripotency of GC-ADO2-iPSCs *in vivo* [20]. SCID Beige mice were purchased from Beijing Vital River Laboratory Animal Technology Co., Ltd. GC-ADO2-iPSCs were resus-

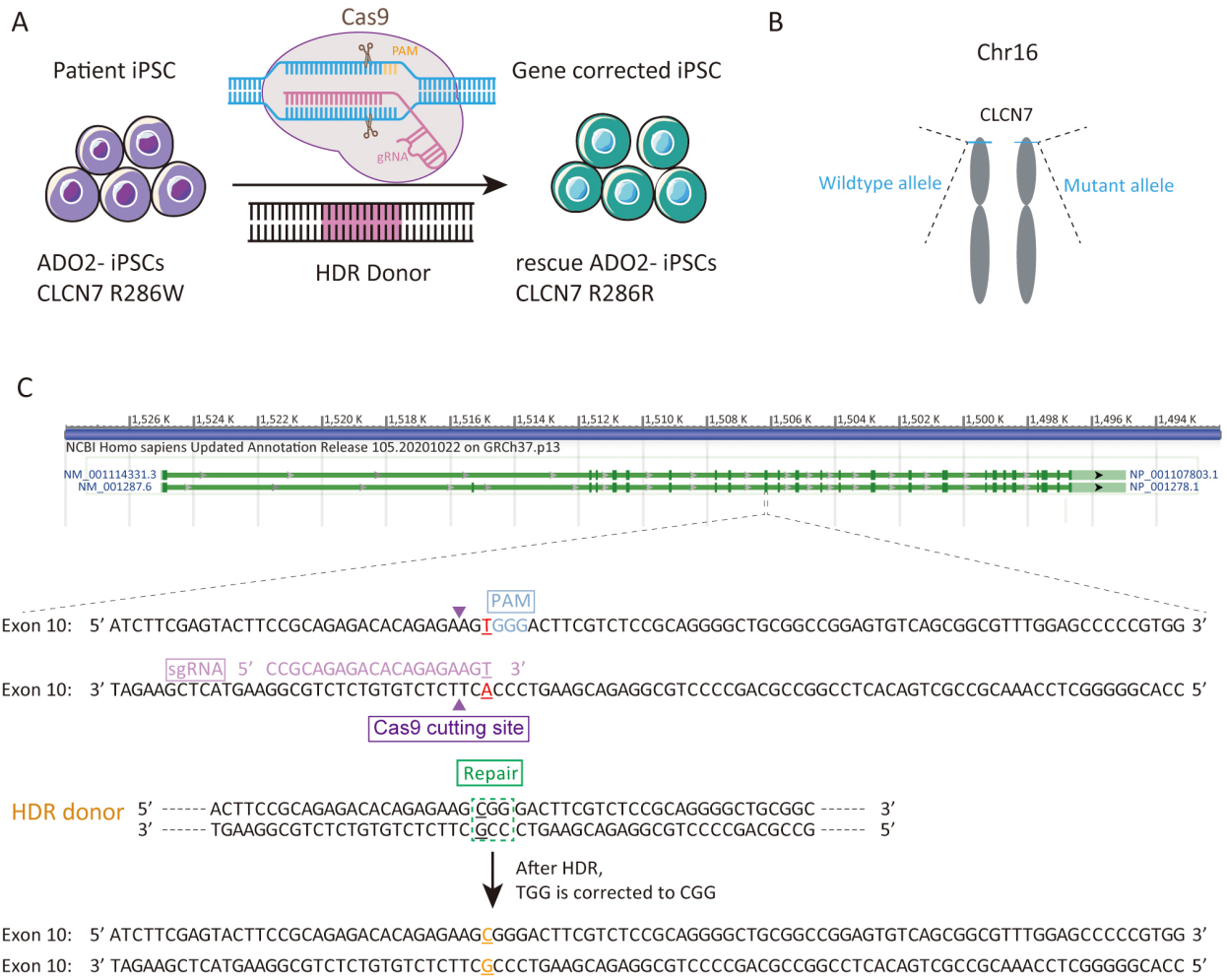

Fig. 1. Experimental design for the correction the R286W mutation of *CLCN7* in ADO2-iPSCs. (A) Schematic representation of gene correction in ADO2-iPSCs. (B) The mutant allele position on the chromosome. (C) Strategy for reversion of the *CLCN7* R286W mutation. The sgRNA sequence was highlighted in pink. PAM was highlighted in blue.

pended in 50% Matrigel (no. 354,277, Corning Inc., Corning, NY, USA) with PBS and injected into the posterior thigh muscles of three 4-weeks-old SCID Beige mice. After 2 months, there is a little protrusion at the injection site and the mice were sacrificed and the tumors were harvested and processed for hematoxylin and eosin (H&E) staining. The other hind leg muscle of the identical mice received an injection of Matrigel in the same volume as a control. Ear tags were used to identify mice.

3. Results

3.1 Specific Targeting of the CLCN7 Gene Using sgRNA-Guided Cas9 Nuclease-Mediated System

We sought to repair the disease causative mutation in osteopetrosis patient-derived iPSCs (ADO2-iPSCs) [20] through in situ gene targeting using CRISPR/Cas9 mediated HDR system (Fig. 1A). The *CLCN7* gene is located at 16p13.3 (Fig. 1B) that encompasses ~30 kb of genomic sequence [22,23]. The mutant exon 10 of *CLCN7* (ATCTTCGAGTACTTCCGCAGAGACACAGAGAAG TGGGACTTCGTCTCCGCAGGGGCTGCGGCCGGAG TGTCAGCGGCGTTTGGAGCCCCCGTGG) was the target for sgRNA design using the design tool (Fig. 1C). The top 5 sgRNAs and their efficiencies were listed in Table 2. One sgRNA (sgRNA5) which overlapped the mutation site of *CLCN7* with the efficiency of 0.646979 was selected as the sgRNA for inducing double-strand breaks (DSBs) near the mutation site. The sgRNA fragment was PCR amplified. The plasmid bearing both Cas9 and sgRNA scaffold backbone (pSpCas9n(BB)-2A-GFP) was used in our study because it could facilitate the fluorescence-based clones screening or selection [21]. The oligo pair encoding the sgRNA sequence was annealed and ligated into the plasmid (pSpCas9n(BB)-2A-GFP) (**Supplementary Fig. 1A**). The donor vector was constructed by cloning the homology arms in the pUC57 plasmid backbone (**Supplementary Fig. 1B**). Upon lipofection with Cas9/sgRNA plasmids and donor vector, iPSCs were cultured under feeder-free conditions.

Table 2. The top 5 sgRNAs.

gRNA ID	Strand	Cut position	gRNA sequence	PAM	Efficiency
sgRNA1	+	30	TCCGCAGAGACACAGAGAAG	TGG	0.681511
sgRNA2	+	49	GTGGGACTTCGTCTCCGCAG	GGG	0.663927
sgRNA3	+	48	AGTGGGACTTCGTCTCCGCA	GGG	0.652291
sgRNA4	+	70	GGCTGCGGCCGGAGTGTCAG	CGG	0.648056
sgRNA5	+	31	CCGCAGAGACACAGAGAAGT	GGG	0.646979

3.2 Confirming Gene Correction

After antibiotic selection using Blasticidin, 11 resistant clones were manually picked and expanded. Their DNAs were extracted and amplified via nested PCR. The resulting amplification products were firstly assessed by agarose gel electrophoresis. As shown in Fig. 2, 10 clones were positive for the targeted 724 bp of amplification product. Clone 15 showing multiple bands was excluded from further sequencing. Two positive clones with site-specific correction of *CLCN7* gene were further confirmed by genomic sequencing (Fig. 3H).

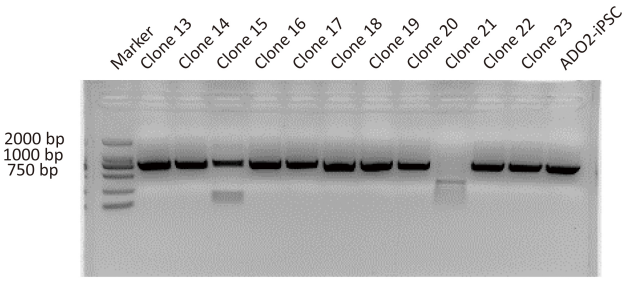

Fig. 2. Representative images showing the PCR assay for *CLCN7* detection in different GC-ADO2-iPSC clones and ADO2-iPSCs. Clone 13-clone23 represent GC-ADO2-iPSC clone 13- GC-ADO2-iPSC clone23.

3.3 Characterization of Gene-Corrected iPSCs

After verified by genomic sequencing, gene-corrected ADO2-iPSCs (GC-ADO2-iPSCs) were expanded on Matrigel-coated plates with a passage every 3–4 days. As shown in Fig. 3A, GC-ADO2-iPSCs resembled a representative hESC morphology including refractive clone edges and high nuclear/cytoplasmic ratio [24]. Chromosome GTG band analysis revealed the chromosome integrity and stability of GC-ADO2-iPSCs with a normal diploid 46, XY karyotype (Fig. 3B), which is consistent with the karyotype analysis result of ADO2-iPSCs [20]. FACS analyses revealed that 99.3% and 98.1% of the cell population of GC-ADO2-iPSCs expressed pluripotency cell surface markers SSEA-4 and TRA1-81 respectively (Fig. 3C,D). In order to check the *in vivo* pluripotency of GC-ADO2-iPSCs, a teratoma formation assay was performed. GC-ADO2-iPSCs were transplanted into SCID Beige mice and the formation of teratomas was observed 8 weeks following the injection. Hematoxylin and eosin staining confirmed that the teratomas had derivatives of all three germ layers, such as the intestinal epithelial cells developed from the endoderm, the cartilage differentiated from the mesoderm, and the neural rosettes formed from the ectoderm (Fig. 3E,F,G). These results revealed the establishment, the pluripotency and multilineage differentiation of GC-ADO2-iPSCs.

To assess the expression of CLCN7, we extracted proteins from the wild-type iPSCs, ADO2-iPSCs, and GC-ADO2-iPSCs. Western blot analysis was performed to determine the relative CLCN7 expression. As shown in Fig. 4A,B, the expression levels of CLCN7 in the wild-type iPSCs, ADO2-iPSCs, and GC-ADO2-iPSCs showed no significant differences, which indicated that c.856C>T (p.R286W) mutation in *CLCN7* exon 10 did not affect the CLCN7 expression in iPSCs.

4. Discussion

The gene *CLCN7* is located at chromosome 16p13.3 in humans having a genomic size of approximate 30 kb [23]. The translation product of this gene, voltage-gated chloride channel 7 (CLCN7), belongs to the CLC chloride channel family of proteins [25]. For mammals, CLCN7 is broadly expressed and mainly distributed in the ruffled membrane of osteoclasts and the membranes of late endosomes and lysosomes [26]. By regulating the balance of Cl^-/H^+ exchange, CLCN7 plays important physiological roles in osteoclasts [25], which plays a central role in the regulation of skeletal bone mass and bone pathologies as large multinucleated bone degrading cells [27]. The pathogenic variants of *CLCN7* gene lead to functional defect of osteoclasts and cause 3 different types of osteopetrosis [28]: infantile malignant *CLCN7*-related recessive osteopetrosis, which is characterized by infancy onset with a severe course, intermediate autosomal recessive osteopetrosis (IARO), whose onset is in childhood and carrying mild clinical manifestations, and autosomal dominant osteopetrosis type II (ADO2), which is manifest in late childhood or adolescence and represents the most common form of osteopetrosis [29]. Biallelic *CLCN7* mutations and single allele *CLCN7* mutations account for severe forms of osteopetrosis and ADO2, respectively. Despite that the mutations in *CLCN7* gene, such as R286W [20], L614R [30], A511P [31], R784W [32], G793R [33], etc., have been intensively studied by virtue of the development of genomic sequenc-

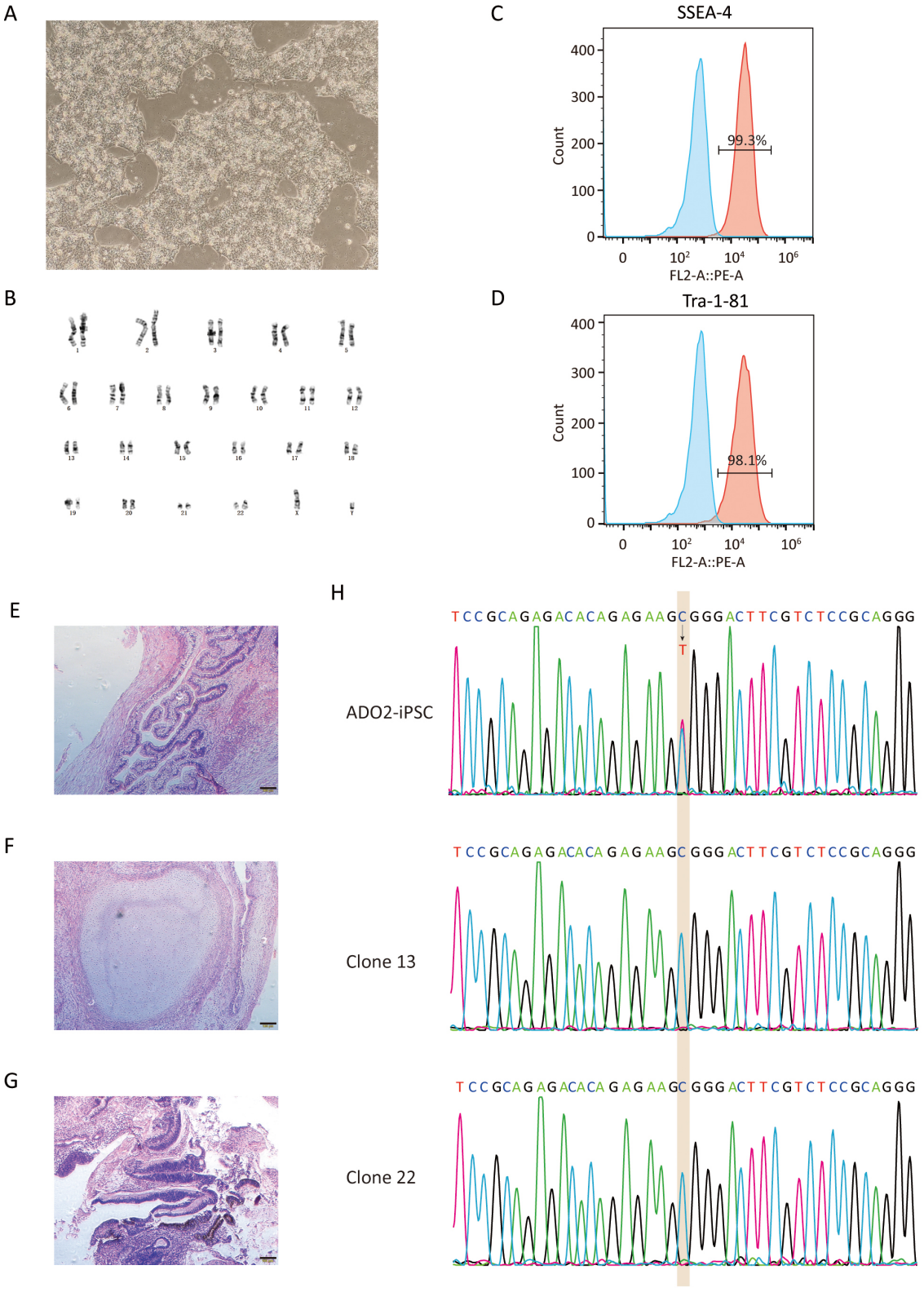

Fig. 3. Characterization of GC-ADO2-iPSCs. (A) Images of GC-ADO2-iPSCs colonies cultured on matrigel. (B) GC-ADO2-iPSCs displayed a normal karyotype. (C,D) Flow cytometric analysis of pluripotency markers SSEA-4 and Tra-1–81 of GC-ADO2-iPSCs. (E,F,G) H&E staining of teratomas derived from immunodeficient mice injected with GC-ADO2-iPSCs shows tissues representing all 3 embryonic germ layers: endoderm (intestinal epithelial cells), mesoderm (cartilage) and ectoderm (neural rosettes). Scale 100 μm. (H) The Sanger sequencing results for clone 13 and clone 22 of GC-ADO2-iPSCs.

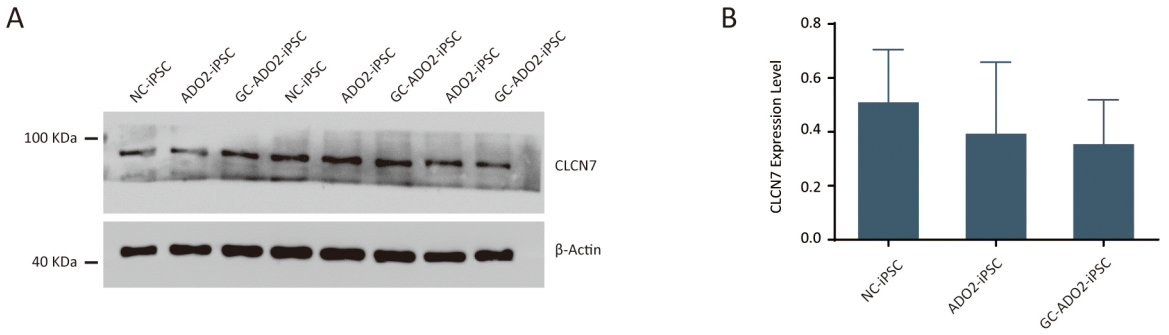

Fig. 4. The expression analysis of CLCN7 in ADO2-iPSC and GC-ADO2-iPSC. (A) Western blotting analysis imaging of CLCN7 in ADO2-iPSC and GC-ADO2-iPSC. (B) Quantification of relative levels of CLCN7 in ADO2-iPSC and GC-ADO2-iPSC. CLCN7 levels were normalized by β-actin (n = 2 or 3).

ing, the precise mechanism of *CLCN7*-related osteopetrosis remains twilight. Therefore, more efforts are necessary to unveil the disease. Osteoclasts from osteopetrosis patients are the ideal reasonable study objects to perform such research. However, such biological samples are extremely precious and the accessibility of such subjects remains a considerable challenge, which have impeded our knowledge of osteopetrosis. Wherefore, it is of great significance and value to establish disease models, which can to some extent more accurately recapitulate disease-associated features.

iPSCs carry the genetic information of their parental cells, possess indefinite propagation ability, have trilineage differentiation potential. Thus, iPSCs provide an ideal platform to investigate the mechanism of various disease, especially of genetic diseases. Up to now, genetic diseases specific iPSCs have become an indispensable research tool for genetic diseases, considerable amounts of which have been successfully established and utilized in mechanistic research and drug estimation. Besides, with the speedy development of genetic engineering techniques, gene corrected patient specific iPSCs, which carry the exact genetic information of their donor cells except disease causative mutation(s), are easy to construct. Benefited from that, they are more appealing as control samples compared with allogeneic healthy samples. Vast quantities of promising results have been reported focusing on genetic corrections of disease-causing genes for elucidating the disease pathology or developing cell or gene therapies.

Previously, rescued bone resorbing activity of the osteoclasts differentiated from gene corrected iPSCs derived from osteopetrotic mice were demonstrated [34]. Another study revealed that the cell function of iPSCs-derived osteoclasts could be rescued by transgenic expression of the functional *TCIRG1* gene to osteopetrotic fibroblasts [35]. A similar study showed that infantile malignant osteopetrosis-specific iPSCs exhibited partially corrected phenotype after transfected a lentiviral vector expressing wild type TCIRG1 [36]. Inspired by these encouraging works, we performed gene correction on ADO2-iPSCs by CRISPR/Cas9 mediated HDR. The assessment performed in our study showed the successful correction of the mutation on *CLCN7* gene in ADO2-iPSCs. The long-term goal of this study is to generate rescued osteoclasts from GC-ADO2-iPSCs and further study *CLCN7* mutations related osteopetrosis pathobiology.

In clinic, HSCT is the only curative for autosomal recessive osteopetrosis [4], which can prevent or reverse most bone-related abnormalities, but has no obvious effect on progressive neurodegeneration [37]. Mesenchymal stem cell transplantation (MSCT) is a considerable strategy to replace the osteoblast precursor population [38]. However, graft versus host disease (GVHD) caused by allogeneic cell transplantation can result in lethal complications. The transplantation of autologous gene-repaired MSC, which derived from gene-repaired patient-derived iPSC, has the advantage of low immunological rejection, which could help to increase the curative rate and reduce costs. The GC-ADO2-iPSCs is a promising seeding cell for autologously treating osteopetrosis. The efficacy of MSCT or HSCT has been evaluated based a number of mouse models of osteopetrosis [39,40]. Thus, it is a recommended study strategy using GC-ADO2-iPSCs derived MSC to treat the mouse models of osteopetrosis. We would like to point out that there is still a long way to applying this method to clinical use, because the tumorigenicity, immunogenicity, and heterogeneity of iPSCs are the most concerning issues [18,41]. Small interfering RNA (siRNA) therapy also showed massive potential for treating osteopetrosis. Anna Teti and her group demonstrated that $Clcn7^{G213R}$-specific siRNA is effective to rescue the ADO2 bone phenotype [42] and cure the extraskeletal manifestations [43]. The long-term safety of this method was also evaluated [44]. Compared with cell therapy, siRNA offers several advantages, as being easy to produce, stable and controllable. The clinical application of siRNA is facing great challenges due to its debatable safety and low bioavailability [45].

Our results demonstrated that iPSCs derived from ADO2 patient could be repaired at the genome level. However, our research presents some limitations. Firstly, the characterization in our study is based on a single gene re-

paired iPSC line. In the future, experimental designs may consider multiple gene repaired iPSC lines to provide more source cells. Secondly, in this study, the function evaluation of GC-ADO2-iPSCs is at on iPSCs stage. Future studies are needed to examine the derived osteoclast from GC-ADO2-iPSCs, since osteoclasts are the most affected cells in osteopetrosis patients.

5. Conclusions

In summary, we successfully corrected the point mutation R286W of the *CLCN7* gene in osteopetrosis iPSCs (ADO2-iPSCs) by CRISPR/Cas9 mediated homologous recombination and obtained the gene corrected cell line GC-ADO2-iPSCs. GC-ADO2-iPSCs had a normal karyotype and expressed pluripotency markers. The wild type sequence of *CLCN7* in GC-ADO2-iPSCs was confirmed by sequencing analysis. GC-ADO2-iPSCs have great potential to offer an attractive resource of isogenic control cellular models for osteopetrosis research.

Abbreviations

ARO, autosomal recessive osteopetrosis; ADO, autosomal dominant osteopetrosis; HSCT, hematopoietic stem cell transplantation; iPSCs, induced pluripotent stem cells; CRISPR/Cas9, clustered regularly interspaced short palindromic repeats-associated 9; ADO2-iPSCs, osteopetrosis-specific iPSCs; GC-ADO2-iPSCs, the gene corrected ADO2-iPSCs; HDR, homology-directed repair; sgRNA, single-guide RNA; IARO, intermediate autosomal recessive osteopetrosis; ADO2, autosomal dominant osteopetrosis type II; CLCN7, chloride channel 7.

Availability of Data and Materials

The data and materials generated during the current study are available from the corresponding author.

Author Contributions

DL—conception and design, data collection, data analysis, manuscript writing, review and editing; MO—conception and design, data collection, financial support, review and editing; WZ—conception, design and review and editing; QL—data analysis, review and editing; WC—data collection, review and editing; CM—Validation, review and editing; WL—Validation, review and editing; GD—data collection, financial support, review and editing; LY—conception and design, supervision, review and editing; PZ—conception and design, data collection, review and editing; DT—conception and design, data collection, review and editing; YD—conception and design, data collection, supervision, financial support, review and editing. All authors have reviewed it critically for important intellectual and approved final manuscript.

Ethics Approval and Consent to Participate

Animal studies were approved by Guilin Medical University Laboratory Animal Ethics Committee (Approval No. GLMC 202003175).

Acknowledgment

We thank the online tool for the single-guide RNA (sgRNA) sequences design (http://www.deephf.com/index/#/cas9).

Funding

This work was supported by the National Natural Science Foundation of China (82060393), the Science and Technology Plan of Shenzhen (JCYJ20180305163846927), the Natural Science Foundation of Guangxi (2020GXNSFAA159124) and the Scientific Research Project of Health System in Pingshan District of Shenzhen (202139). And all the fundings did not involve in the design of the study and collection, analysis, and interpretation of data and in writing the manuscript.

Conflict of Interest

The authors declare no conflict of interest.

Supplementary Material

Supplementary material associated with this article can be found, in the online version, at https://doi.org/10.31083/j.fbl2806131.

References

[1] Sobacchi C, Schulz A, Coxon FP, Villa A, Helfrich MH. Osteopetrosis: genetics, treatment and new insights into osteoclast function. Nature Reviews. Endocrinology. 2013; 9: 522–536.

[2] Teti A, Econs MJ. Osteopetroses, emphasizing potential approaches to treatment. Bone. 2017; 102: 50–59.

[3] Tolar J, Teitelbaum SL, Orchard PJ. Osteopetrosis. The New England Journal of Medicine. 2004; 351: 2839–2849.

[4] Penna S, Villa A, Capo V. Autosomal recessive osteopetrosis: mechanisms and treatments. Disease Models & Mechanisms. 2021; 14: dmm048940.

[5] Segovia-Silvestre T, Neutzsky-Wulff AV, Sorensen MG, Christiansen C, Bollerslev J, Karsdal MA, *et al*. Advances in osteoclast biology resulting from the study of osteopetrotic mutations. Human Genetics. 2009; 124: 561–577.

[6] Trajanoska K, Rivadeneira F. Genomic Medicine: Lessons Learned from Monogenic and Complex Bone Disorders. Frontiers in Endocrinology. 2020; 11: 556610.

[7] Karasik D, Rivadeneira F, Johnson ML. The genetics of bone mass and susceptibility to bone diseases. Nature Reviews. Rheumatology. 2016; 12: 323–334.

[8] Palagano E, Menale C, Sobacchi C, Villa A. Genetics of Osteopetrosis. Current Osteoporosis Reports. 2018; 16: 13–25.

[9] Wu CC, Econs MJ, DiMeglio LA, Insogna KL, Levine MA, Orchard PJ, *et al*. Diagnosis and Management of Osteopetrosis: Consensus Guidelines from the Osteopetrosis Working Group. The Journal of Clinical Endocrinology and Metabolism. 2017; 102: 3111–3123.

[10] Sharma A, Sances S, Workman MJ, Svendsen CN. Multi-lineage

Human iPSC-Derived Platforms for Disease Modeling and Drug Discovery. Cell Stem Cell. 2020; 26: 309–329.
[11] Rowe RG, Daley GQ. Induced pluripotent stem cells in disease modelling and drug discovery. Nature Reviews. Genetics. 2019; 20: 377–388.
[12] De Luca M, Aiuti A, Cossu G, Parmar M, Pellegrini G, Robey PG. Advances in stem cell research and therapeutic development. Nature Cell Biology. 2019; 21: 801–811.
[13] Yun Y, Ha Y. CRISPR/Cas9-Mediated Gene Correction to Understand ALS. International Journal of Molecular Sciences. 2020; 21: 3801.
[14] Pickar-Oliver A, Gersbach CA. The next generation of CRISPR-Cas technologies and applications. Nature Reviews. Molecular Cell Biology. 2019; 20: 490–507.
[15] Jiang F, Doudna JA. CRISPR-Cas9 Structures and Mechanisms. Annual Review of Biophysics. 2017; 46: 505–529.
[16] Dhoke NR, Kim H, Selvaraj S, Azzag K, Zhou H, Oliveira NAJ, *et al*. A universal gene correction approach for FKRP-associated dystroglycanopathies to enable autologous cell therapy. Cell Reports. 2021; 36: 109360.
[17] Selvaraj S, Dhoke NR, Kiley J, Mateos-Aierdi AJ, Tungtur S, Mondragon-Gonzalez R, *et al*. Gene Correction of LGMD2A Patient-Specific iPSCs for the Development of Targeted Autologous Cell Therapy. Molecular Therapy: the Journal of the American Society of Gene Therapy. 2019; 27: 2147–2157.
[18] Yamanaka S. Pluripotent Stem Cell-Based Cell Therapy-Promise and Challenges. Cell Stem Cell. 2020; 27: 523–531.
[19] Soldner F, Jaenisch R. Stem Cells, Genome Editing, and the Path to Translational Medicine. Cell. 2018; 175: 615–632.
[20] Ou M, Li C, Tang D, Xue W, Xu Y, Zhu P, *et al*. Genotyping, generation and proteomic profiling of the first human autosomal dominant osteopetrosis type II-specific induced pluripotent stem cells. Stem Cell Research & Therapy. 2019; 10: 251.
[21] Ran FA, Hsu PD, Wright J, Agarwala V, Scott DA, Zhang F. Genome engineering using the CRISPR-Cas9 system. Nature Protocols. 2013; 8: 2281–2308.
[22] Waguespack SG, Koller DL, White KE, Fishburn T, Carn G, Buckwalter KA, *et al*. Chloride channel 7 (ClCN7) gene mutations and autosomal dominant osteopetrosis, type II. Journal of Bone and Mineral Research: the Official Journal of the American Society for Bone and Mineral Research. 2003; 18: 1513–1518.
[23] Zhang S, Liu Y, Zhang B, Zhou J, Li T, Liu Z, *et al*. Molecular insights into the human CLC-7/Ostm1 transporter. Science Advances. 2020; 6: eabb4747.
[24] Lowry WE, Richter L, Yachechko R, Pyle AD, Tchieu J, Sridharan R, *et al*. Generation of human induced pluripotent stem cells from dermal fibroblasts. Proceedings of the National Academy of Sciences of the United States of America. 2008; 105: 2883–2888.
[25] Ribet ABP, Ng PY, Pavlos NJ. Membrane Transport Proteins in Osteoclasts: The Ins and Outs. Frontiers in Cell and Developmental Biology. 2021; 9: 644986.
[26] Barrallo-Gimeno A, Gradogna A, Zanardi I, Pusch M, Estévez R. Regulatory-auxiliary subunits of CLC chloride channel-transport proteins. The Journal of Physiology. 2015; 593: 4111–4127.
[27] Novack DV, Mbalaviele G. Osteoclasts-Key Players in Skeletal Health and Disease. Microbiology Spectrum. 2016; 4: 235.
[28] Frattini A, Pangrazio A, Susani L, Sobacchi C, Mirolo M, Abinun M, *et al*. Chloride channel ClCN7 mutations are responsible for severe recessive, dominant, and intermediate osteopetrosis. Journal of Bone and Mineral Research: the Official Journal of the American Society for Bone and Mineral Research. 2003; 18: 1740–1747.
[29] Bollerslev J, Henriksen K, Nielsen MF, Brixen K, Van Hul W. Autosomal dominant osteopetrosis revisited: lessons from recent studies. European Journal of Endocrinology. 2013; 169: R39–R57.
[30] Bug DS, Barkhatov IM, Gudozhnikova YV, Tishkov AV, Zhulin IB, Petukhova NV. Identification and Characterization of a Novel *CLCN7* Variant Associated with Osteopetrosis. Genes. 2020; 11: 1242.
[31] Stepensky P, Grisariu S, Avni B, Zaidman I, Shadur B, Elpeleg O, *et al*. Stem cell transplantation for osteopetrosis in patients beyond the age of 5 years. Blood Advances. 2019; 3: 862–868.
[32] Deng H, He D, Rong P, Xu H, Yuan L, Li L, *et al*. Novel CLCN7 mutation identified in a Han Chinese family with autosomal dominant osteopetrosis-2. Molecular Pain. 2016; 12: 1744806916652628.
[33] Li L, Lv SS, Wang C, Yue H, Zhang ZL. Novel CLCN7 mutations cause autosomal dominant osteopetrosis type II and intermediate autosomal recessive osteopetrosis. Molecular Medicine Reports. 2019; 19: 5030–5038.
[34] Neri T, Muggeo S, Paulis M, Caldana ME, Crisafulli L, Strina D, *et al*. Targeted Gene Correction in Osteopetrotic-Induced Pluripotent Stem Cells for the Generation of Functional Osteoclasts. Stem Cell Reports. 2015; 5: 558–568.
[35] Chen W, Twaroski K, Eide C, Riddle MJ, Orchard PJ, Tolar J. TCIRG1 Transgenic Rescue of Osteoclast Function Using Induced Pluripotent Stem Cells Derived from Patients with Infantile Malignant Autosomal Recessive Osteopetrosis. The Journal of Bone and Joint Surgery. American Volume. 2019; 101: 1939–1947.
[36] Xian X, Moraghebi R, Löfvall H, Fasth A, Henriksen K, Richter J, *et al*. Generation of gene-corrected functional osteoclasts from osteopetrotic induced pluripotent stem cells. Stem Cell Research & Therapy. 2020; 11: 179.
[37] Cohen-Solal M, Collet C, Bizot P, Pavis C, Funck-Brentano T. Osteopetrosis: The patient point of view and medical challenges. Bone. 2023; 167: 116635.
[38] Penna S, Capo V, Palagano E, Sobacchi C, Villa A. One Disease, Many Genes: Implications for the Treatment of Osteopetroses. Frontiers in Endocrinology. 2019; 10: 85.
[39] Alam I, Gerard-O'Riley RL, Acton D, Hardman SL, Murphy M, Alvarez MB, *et al*. Bone marrow transplantation as a therapy for autosomal dominant osteopetrosis type 2 in mice. FASEB Journal: Official Publication of the Federation of American Societies for Experimental Biology. 2022; 36: e22471.
[40] Chalhoub N, Benachenhou N, Rajapurohitam V, Pata M, Ferron M, Frattini A, *et al*. Grey-lethal mutation induces severe malignant autosomal recessive osteopetrosis in mouse and human. Nature Medicine. 2003; 9: 399–406.
[41] Sinenko SA, Ponomartsev SV, Tomilin AN. Pluripotent stem cell-based gene therapy approach: human de novo synthesized chromosomes. Cellular and Molecular Life Sciences: CMLS. 2021; 78: 1207–1220.
[42] Capulli M, Maurizi A, Ventura L, Rucci N, Teti A. Effective Small Interfering RNA Therapy to Treat CLCN7-dependent Autosomal Dominant Osteopetrosis Type 2. Molecular Therapy. Nucleic Acids. 2015; 4: e248.
[43] Maurizi A, Capulli M, Curle A, Patel R, Ucci A, Côrtes JA, *et al*. Extra-skeletal manifestations in mice affected by *Clcn7*-dependent autosomal dominant osteopetrosis type 2 clinical and therapeutic implications. Bone Research. 2019; 7: 17.
[44] Maurizi A, Capulli M, Patel R, Curle A, Rucci N, Teti A. RNA interference therapy for autosomal dominant osteopetrosis type 2. Towards the preclinical development. Bone. 2018; 110: 343–354.
[45] Friedrich M, Aigner A. Therapeutic siRNA: State-of-the-Art and Future Perspectives. BioDrugs: Clinical Immunotherapeutics, Biopharmaceuticals and Gene Therapy. 2022; 36: 549–571.